Journal of Orthopaedic Translation 29 (2021) 113–122

Contents lists available at ScienceDirect

Journal of Orthopaedic Translation

journal homepage: www.journals.elsevier.com/journal-of-orthopaedic-translation

Unilateral cervical spinal cord injury induces bone loss and metabolic changes in non-human primates (*Macaca fascicularis*)

Xiuhua Wu [a,1], Xiaolin Xu [b,1], Qi Liu [a], Jianyang Ding [a], Junhao Liu [a], Zhiping Huang [a], Zucheng Huang [a], Xiaoliang Wu [a], Rong Li [a], Zhou Yang [a], Hui Jiang [a], Jie Liu [c], Qingan Zhu [a,*]

[a] *Division of Spine Surgery, Department of Orthopaedics, Nanfang Hospital, Southern Medical University, Guangzhou, Guangdong, China*
[b] *Department of Surgery, Peking Union Medical College Hospital, Chinese Academy of Medical Sciences, Beijing, China*
[c] *International Collaboration on Repair Discoveries (ICORD), Blusson Spinal Cord Center, Vancouver, BritishColumbia, Canada*

ARTICLE INFO

Keywords:
Osteoporosis
Spinal cord injury
Bone microarchitecture
Non-human primates (NHP)

ABSTRACT

Background/Objective: The deleterious effects of chronic spinal cord injury (SCI) on the skeleton in rats, especially the lower extremities, has been proved previously. However, the long-term skeletal changes after SCI in non-human primates (NHP) have been scarcely studied. This study aimed to evaluate the bone loss in limbs and vertebrae and the bone metabolic changes in NHP after unilateral cervical spinal cord contusion injury.

Methods: Twelve *Macaca fascicularis* were randomly divided into the SCI (n=8) and the Sham (n=4) groups. The SCI models were established using hemi-contusion cervical spinal cord injury on fifth cervical vertebra (C5), and were further evaluated by histological staining and neurophysiological monitoring. Changes of bone microstructures, bone biomechanics, and bone metabolism markers were assessed by micro-CT, micro-FEA and serological kit.

Results: The NHP hemi-contusion cervical SCI model led to consistent unilateral limb dysfunction and potential plasticity in the face of loss of spinal cord. Furthermore, the cancellous bone mass of ipsilateral humerus and radius decreased significantly compared to the contralateral side. The bone volume fraction of humerus and radius were 17.2% and 20.1% on the ipsilateral while 29.0% and 30.1% on the contralateral respectively. Similarly, the thickness of the cortical bone in the ipsilateral forelimbs was significantly decreased, as well as the bone strength of the ipsilateral forelimbs. These changes were accompanied by diminished concentration of osteocalcin and total procollagen type 1 N-terminal propeptide (t-P1NP) as well as increased level of β-C-terminal cross-linking telopeptide of type 1collagen (β-CTX) in serological testing.

Conclusions: The present study demonstrated that hemi-SCI induced loss of bone mass and compromised biomechanical performance in ipsilateral forelimbs, which could be indicated by both muscle atrophy and serological changes of bone metabolism, and associated with a consistent loss of large-diameter cells of sensory neurons in the dorsal root ganglia.

The Translational potential of this Article: Our study, for the first time, demonstrated the bone loss in limbs and vertebrae as well as the bone metabolic changes in non-human primates after unilateral spinal cord injury (SCI). This may help to elucidate the role of muscle atrophy, serological changes and loss of sensory neurons in the mechanisms of SCI-induced osteoporosis, which would be definitely better compared with rodent models.

Introduction

As one of the most common and debilitating conditions that has been observed in almost every patient with spinal cord injury (SCI), osteoporosis is characterized by low bone mass and deterioration of microarchitectures, resulting in increased bone fragility and susceptibility to fractures [1]. Different from postmenopausal osteoporosis which favors fractures in the vertebrae, hip, and wrist bones [2], osteoporosis induced by SCI exhibits a unique rate of distribution and resistance to currently available treatments [1]. After SCI, significant bone loss was

* Corresponding author. Division of Spine Surgery, Department of Orthopaedics, Nanfang Hospital, Southern Medical University, 1838 North Guangzhou Avenue, Guangzhou, 510515, PR China.
E-mail address: qinganzhu@gmail.com (Q. Zhu).
[1] These authors contributed equally to this work and should be considered co-first authors.

https://doi.org/10.1016/j.jot.2021.03.006
Received 28 June 2020; Received in revised form 14 November 2020; Accepted 1 March 2021

usually observed in sublesional long bones, in which areas around trabecular epiphyseal and metaphyseal sections of the distal femur and proximal tibia were affected maximally [3]. Clinical studies have proved a high prevalence of lower extremity fractures ranging from 1 to 34% among individuals with SCI [4], while no demineralization in the spine and supralesional areas has been noticed [5].

One of the major factors in the pathogenesis of SCI-induced osteoporosis is mechanical unloading based on the loss of motor function [3]. The sublesional muscle atrophy and loss of contractions may weaken the loading forces, resulting in the deterioration of bone geometry and structures [6]. Meanwhile, denervation may also play a key role in the situation. The loss of positive neural innervation to the sublesional skeleton may primarily contribute to the rapidity and magnitude of bone loss after SCI. Other possible mediating factors may include metabolic, endocrine, and vascular changes [5]. Although cervical SCI is the most common type of traumatic SCI clinically [7], the majority of previous laboratory research employs paraplegic rodent models for thoracic cord injury [8] and focus on the changes of sublesional long bones [9]. Non-human primates (NHP) models, which demonstrate high genetic, biological, and physiological similarities with humans, would definitely be better in the study of SCI-induced osteoporosis compared with rodent models.

In order to characterize the microstructures and biomechanical properties of upper limb long bones as well as vertebrae after cervical hemi-SCI, the present study managed to establish a unilateral cervical cord contusion model using *Macaca fascicularis*. The microstructures of humerus, radius, and the 4th lumbar vertebrae as well as the biomechanical properties, serological bone turnover markers, were all compared and analyzed.

Methods

Hemi-contusion surgical procedure

A total of 12 adult male *M. fascicularis* with a mean age of 7.5 ± 1.6 years (provided by Guangdong Landau Biotechnology Co. Ltd) were randomly divided into two groups: the Sham group (n = 4) and the SCI group (n = 8). The SCI group received hemi-contusion cervical cord injury and was observed for 6 months (n = 4) and 12 months (n = 4) respectively, while the Sham group was observed for a total of 12 months.

The cervical cord injury procedure was conducted according to previous studies [10–12] and consistent with our published research [13]. A laminectomy was performed to expose the C5 spinal cord, and the vertebral column was secured with a self-designed clamp to the C4–C6 site. A impactor tip with a diameter of 4 mm was initially lowered to contact the dura with a contact force of 0.2 N. Then the impactor tip was driven by a servo-electromagnetic material testing machine (E1000 Electro PlusTM; Instron Inc., MA) into the left side of the C5 spinal cord at a speed of 800 mm/s and a displacement of 4.0–4.5 mm. During the surgery, body temperature, heart rate, respiration rate and indirect blood pressure were monitored closely.

All animal procedures were approved by the Committee on the Ethics of Animal Experiments of our institute and conducted in accordance with the guidelines for the care of laboratory animals.

Electrophysiological assessment

The motor evoked potential (MEPs) and somatosensory evoked potential (SSEPs) signals of the *M. fascicularis* were collected 20weeks post-SCI and compared between the Sham and SCI groups using a 16-channel neuromonitoring system (YRKJ-G2008; Zhuhai, China). The animals were firstly anesthetized with ketamine (5–10 mg/kg) intramuscular injection and then anesthetized with sodium pentobarbital (10 mg/kg) administered intravenously. The core temperature was maintained at 37.5 °C using a homeothermic blanket. The scalp was shaved and disinfected with 70% alcohol.

During the electrophysiological recording, needle electrodes were inserted into the thenar muscle of the forelimbs. The stimulus intensity of 30–50 mA that elicited a motor evoked potential (MEP) with a pulse width of 1 msec at a frequency of 300 Hz was established. The peak-to-peak amplitudes of MEPs from three stimulations were recorded to assess the intra-animal variability and reproducibility. The SSEPs were evoked continuously by sensory stimulation delivered via two needle electrodes inserted into the forelimbs bilaterally adjacent to the median nerve. In addition, a reference electrode was placed subcutaneously over the skull at the central midline and at frontal midline. Constant current pulses (5–10 mA, 0.20 ms) were delivered at a frequency of 5.3 Hz to obtained the SSEPs signals. Finally, the 300 responses of SSEPs were averaged for each trial to obtain an optimal signal-to-noise ratio for the SSEP signals.

Hematoxylin-eosin (HE) Staining of Spinal Cord

Before decapitation, *M. fascicularis* were anesthetized with sodium pentobarbital and perfused transcardially with 0.1 M phosphate-buffered saline (PBS) followed by ice-cold 4% paraformaldehyde. Subsequently, the spinal cord was collected, fixed overnight in 4% paraformaldehyde, and cryoprotected in graded series of sucrose. Then, the tissue was sectioned into 20-μm-thick slices using a microtome cryostat (Leica, Germany) in the cross-section plane, follows by HE staining for examination.

Bone length and dry weight of muscles

The bone length of the ulna, radius, and humerus between the groups were measured using a Vernier calipers (precision of 0.01 mm).

In order to compare the difference of muscle mass in the forelimbs after spinal cord injury, the tissue was dried in an incubator under 55 °C for 24 h and the weight of forearm muscles including the musculi palmaris longus (MPL), the brachioradialis (BR), the pronator teres (PT), and the flexor carpi radialis (FCR) were measured using CS 200 weighing balance (Ohaus, Pine Brook, NJ, USA).

Micro-CT analysis

The long bones of upper limbs including the humerus and radius were dissected carefully and fixed in 4% paraformaldehyde for 48 h. The specimens were attached to a small cystosepiment and kept straight in the micro-CT tube. A high-resolution micro-CT system (μCT 80, Scanco Medical, AG, Switzerland) was used to scan the proximal humerus, the mid-shaft humerus, the distal radius, and the fourth lumbar vertebrae (L4) with an isotropic voxel size of 36 μm (55 kv, 145 μA, integration time 300 ms, averaged two times). Cancellous bone, including the proximal humerus, the distal radius and the fourth lumbar vertebrae (L4), with cortical bone, including the mid-shaft humerus and the distal radius, were selected for bone microarchitecture analysis. The metaphyseal region of the proximal humerus and distal radius within a rectangular area 2 mm distal from the central point of the growth plate–metaphyseal junction, as well as the whole 4th vertebrae were possessed for both cancellous and cortical bone evaluation.

Parameters including bone volume/tissue volume (BV/TV), trabecular number (Tb.N), trabecular thickness (Tb.Th), trabecular separation (Tb.Sp), connectivity density (Conn.D), and bone mineral density (BMD) were used to evaluate cancellous bone, while total cross-sectional area inside the periosteal envelope (Tarea), bone area (Barea), and bone thickness (Ct.Th) were applied for cortical bone assessment. All these data were collected using the software provided by the manufacturer.

Micro-finite element (micro-FE) evaluation

To evaluate the biomechanical properties of the proximal humerus

and distal radius (including both cancellous and cortical bone), the compressive test was performed using micro-FE analysis software (Scanco Medical AG, version 1.13) based on the reconstructed structure using three-dimensional micro-CT images as described previously [14]. Briefly, the bone tissue was modeled as an isotropic and linear elastic material with a Poisson's ratio of $\nu = 0.3$ and Young's modulus of material = 10,000 MPa. The simulation yielded compressive stiffness and failure load of bones.

Serological measurement

After anesthesia, 10 mL venous blood were obtained from each subject. The blood samples were left at room temperature for 2 h and then centrifuged at 3000 rpm for 20 min to acquire the serum samples. The serological calcium, phosphorus, and Vitamin D concentrations, as well as the levels of specific markers of bone turnover, including bone-specific alkaline phosphatase (ALP), osteocalcin (OCN), total N-terminal propeptide of type I procollagen (t-P1NP), and C-telopeptide fragments of collagen type I a1 chains (β-CTX), were measured using the kits (Beckman Coulter, Suzhou, China) according to the manufacturer's protocols.

Statistical analysis

Statistical analysis was performed using the SPSS v.20 software (SPSS Inc., IL, USA), and all data are expressed as means ± standard deviation. The data within the groups were compared using paired-samples *t*-test, while the data between the groups were compared using independent-samples *t*-test. $P < 0.05$ was considered statistically significant for all tests.

Results

Successful establishment of the hemi-contusion SCI model

The ipsilateral spinal cord was severely damaged with loss of the ventral horns of gray matter and lateral funiculus of the white matter at the epicenter of the striking point (Fig. 1A). Moreover, the electrophysiological monitoring altered significantly after SCI, wherein the ipsilateral MEPs and SEPs showed latency prolongation and amplitude reduction (Fig. 1B). The histological and electrophysiological changes designated the successful establishment of the unilateral cervical spinal cord contusion model in *M. fascicularis*.

Changes in bone length and atrophy of muscles after SCI

The length of the ulna, radius, and humerus did not show any difference between the ipsilateral and contralateral sides or between groups (Table 1). However, a rapid and dramatic loss of muscle mass was observed in the forelimb on the ipsilateral side as compared to the contralateral side after SCI (Fig. 2). The dry weight of the MPL, FCR, PT, and BR decreased by 36.8%, 39.8%, 52.3%, and 32.4% respectively compared with the uninjured side in the SCI group. When compared to the sham group, the dry weight of MPL, FCR and PT was significantly reduced in the ipsilateral side after SCI (sham *vs*. SCI: 0.73 ± 0.15 *vs*. 0.35 ± 0.11 g, $P = 0.0062$; 1.70 ± 0.3 *vs*. 0.67 ± 0.41 g, $P = 0.0079$; 1.80 ± 0.36 *vs*. 0.73 ± 0.47 g, $P = 0.0114$, respectively). The dry weight of the BR did not show any difference between the two groups.

Bone micro-architectural impairment in the forelimbs after SCI

At the growth plate–metaphyseal junction of the proximal humerus and distal radius, the bone mass reduced on the ipsilateral side after SCI. The BMD of the proximal humerus and distal radius decreased by 43.9% and 38.0% in the ipsilateral side than that in the contralateral side. The ipsilateral proximal humerus showed lower BV/TV ($p = 0.002$), Tb.N ($p = 0.007$), and Tb.Th ($p = 0.035$) and higher Tb. Sp ($p = 0.055$) in the ipsilateral side than that in the contralateral side (Fig. 3). Similarly, SCI significantly decreased BV/TV ($p < 0.001$), Tb.N ($p = 0.001$), and Tb.Th ($p = 0.004$) and increased Tb. Sp ($p = 0.001$) in the ipsilateral distal radius when compared to that on the contralateral side (Fig. 4). Interestingly, among all the cancellous bone parameters, only BV/TV of the distal radius demonstrated significant difference ($p = 0.042$) between the sham and SCI groups on the ipsilateral side, no other significance was found between two groups. In addition, for vertebral cancellous bone, the

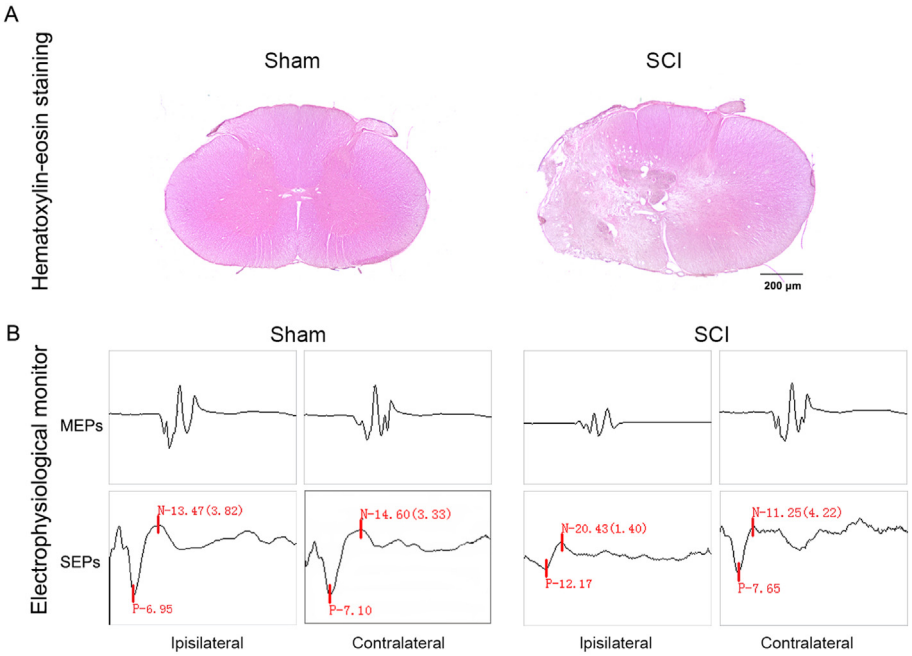

Fig. 1. Successful established the hemi-contusion SCI Model in NHP. **A** The HE staining of spinal cord tissue in the transverse section after 6 months injury. The spinal cord at the epicenter of ipsilateral was severe damage after SCI, with loss of the ventral horns of gray matter and lateral funiculus of white matter. **B** The electrophysiological monitoring after 6 months injury. The ipsilateral MEPs and SEPs were showed latency prolongation and amplitude reduction after SCI.

Table 1
The bone length of humerus, radius and ulna after SCI.

	Humerus		Radius		Ulna	
	Ipsilateral	Contralateral	Ipsilateral	Contralateral	Ipsilateral	Contralateral
Sham	141.0 ± 11.1	140.9 ± 11.5	141.8 ± 11.4	141.5 ± 11.4	160.7 ± 12.4	159.7 ± 11.5
SCI	135.5 ± 6.3	137.4 ± 5.8	136.2 ± 4.0	135.7 ± 4.3	152.6 ± 3.7	152.7 ± 4.8

Note: Data are expressed as means ± SD (n = 4 in the sham group and n = 8 in the SCI group)

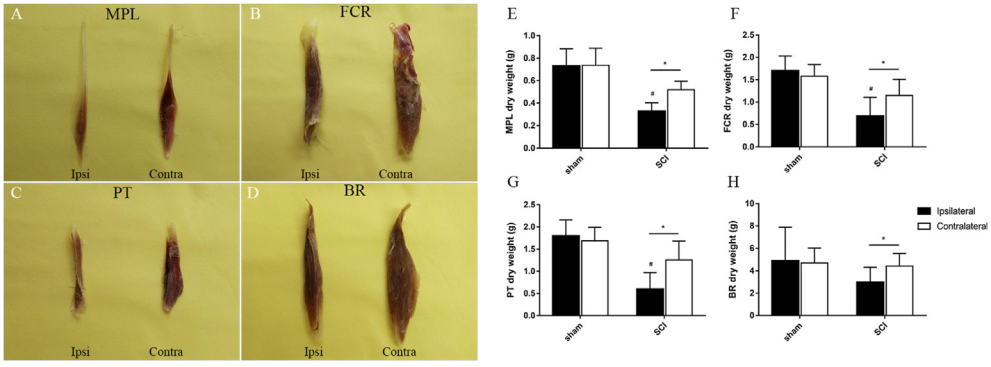

Fig. 2. Atrophy of muscles in forelimb after SCI. **A-D** The musculi palmaris longus (MPL), flexor carpi radialis (FCR), pronator teres (PT) and brachioradialis (BR) were marked atrophy between ipsilateral and contralateral sides after SCI. **E-F** The dry weight of MPL, FCR, PT and BR between ipsilateral and contralateral sides or control and SCI groups after injury. *P < 0.05 between the ipsilateral side and contralateral side, #P < 0.05 between the control group and SCI group (control, n = 4; SCI, n = 8)

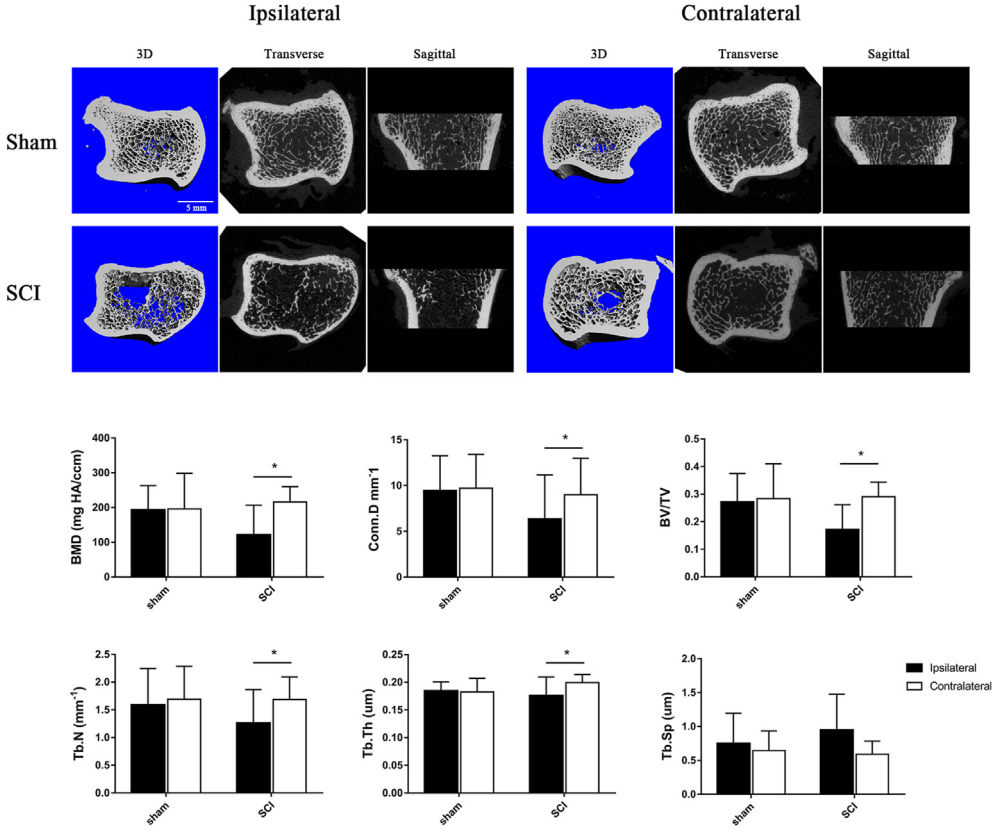

Fig. 3. The bone microstructure change of cancellous bone in the proximal humerus. **A** The 3D images of transverse section and the 2D images of transverse and sagittal sections. B The trabecula parameters of cancellous bone. *P < 0.05 between the ipsilateral side and contralateral side (control, n = 4; SCI, n = 8)

BMD between SCI and sham groups was 207.2 mg HA/ccm and 233.9 mg HA/ccm, and the BV/TV was 29.8% and 35.9% respectively. Although the SCI group somehow showed compromised trabecular structure than the sham group, no difference was observed in all the cancellous parameters between two groups ($p > 0.05$) (Fig. 5).

The cortical bone was also affected. The cortical thickness on the ipsilateral side of SCI was slimmer than that of the contralateral side. In the mid-shaft humerus, Barea, Tarea, and Ct. Th decreased by 9.5%, 3.1%, and 21.1% respectively on the ipsilateral side in the SCI group, which showed remarkable difference compared to the contralateral side (Fig. 6). The distal radius also showed dramatically decrease in Barea ($p = 0.022$), Tarea ($p = 0.009$), and Ct. Th ($p = 0.001$) in the ipsilateral side

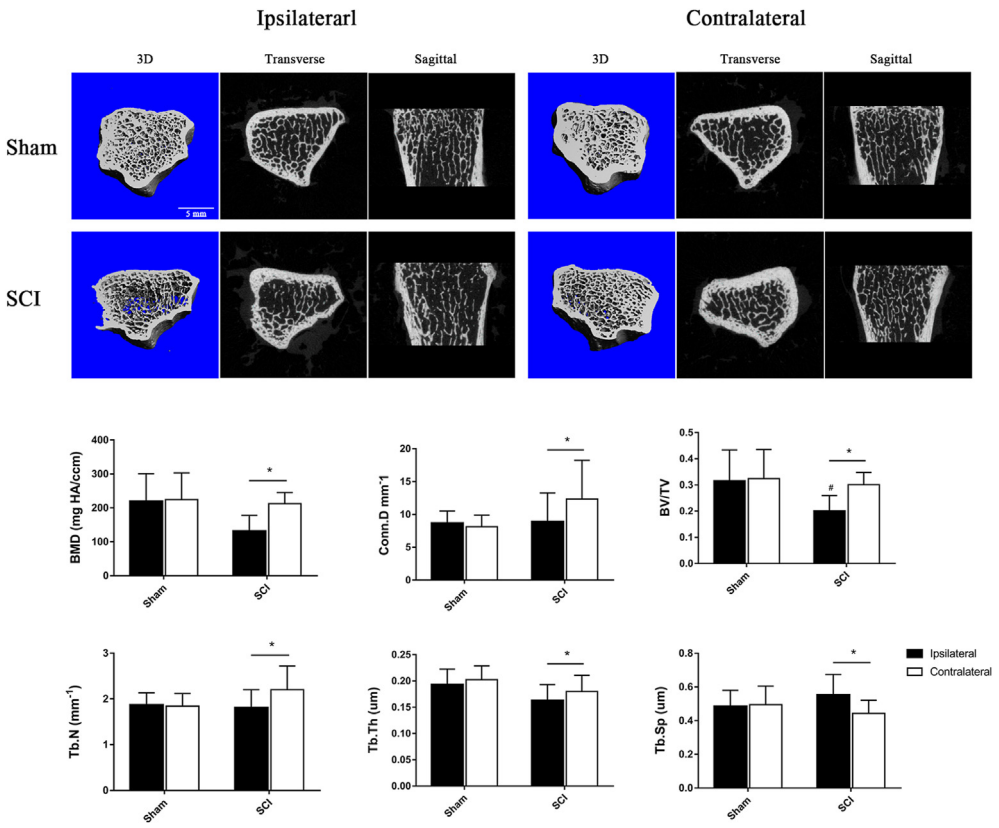

Fig. 4. The bone microstructure change of cancellous bone in the distal radius. **A** The 3D images of transverse section and the 2D images of transverse and sagittal sections. B The trabecula parameters of cancellous bone. *P < 0.05 between the ipsilateral side and contralateral side, #P < 0.05 between the control group and SCI group (control, n = 4; SCI, n = 8)

after SCI. When compared to the sham group, the Tarea of the radius decreased significantly after SCI in both sides (sham *vs.* SCI: 32.7 *vs.* 24.6 mm^2 and 33.9*vs.* 27.2 mm^2, respectively). Also, the Ct. Th in the ipsilateral radius was thinner ($p = 0.03$) in the SCI group than that in the sham group (Fig. 7).

Bone biomechanics weakened in forelimbs after SCI

The biomechanical properties of the proximal humerus and distal radius were significantly weakened by spinal cord contusion. In the SCI group, the stiffness of the humerus and radius decreased by 28.9% and 36.6% in the ipsilateral side when compared to the contralateral side, and the failure load reduced by 27.2% and 40.2% respectively. Similarly, the stiffness and failure load of humerus and radius reduced significantly in the ipsilateral side in the SCI group as compared to that in the sham group ($p < 0.05$). However, the stiffness and failure load of L4 vertebrae did not show any distinction between the groups (sham *vs.* SCI: $41.2 \pm 9.2 \times 10^4$ N/m *vs.* $32.7 \pm 1.5 \times 10^4$ N/m and $2.2 \pm 0.7 \times 10^2$ *vs.* $2.0 \pm 0.2 \times 10^2$ N/m, respectively) (Table 2).

Serological biomarker outcomes

The serological levels of calcium, phosphorus, and Vitamin D were 2.22 and 2.34 mmol/L, 1.04 and 1.75 mmol/L, and 122.3 and 118.0 ng/mL in the sham and SCI groups respectively, no significant differences were found between groups ($p > 0.05$) (Table 3). After SCI, the serological levels of ALP and β-CTX increased by 15.9% and 12.5%, while those of OCN and t-P1NP decreased by 34.1% and 48.6%, respectively. However, the bone turnover markers did not show any statistical difference between two groups either ($p > 0.05$) (Table 3).

Discussion

Bone loss or osteoporosis is one of the most common and debilitating conditions after SCI, which may greatly increase the risk of fractures [15]. In the present study, we managed to establish a hemi-contusion cervical SCI model using NHP (*M. fascicularis*), after which the bone microstructures and biomechanics on both the ipsilateral and contralateral sides of SCI in forelimbs were comprehensively analyzed. The bone length, muscle mass and serological bone turnover biomarkers were also monitored and compared. In this model, we confirmed that the hemi-contusion SCI decreased the bone mass and weakened the biomechanical properties in the ipsilateral humerus and radius, it also attenuated cortical bone thickness and lead to sparse trabeculae structures. In addition, on the ipsilateral side of the spinal contusion, the muscles of the upper extremities exhibited significant atrophy, the bone formation markers decreased while the absorption markers increased compared with the contralateral side.

Previous studies on bone loss after SCI primarily focused on thoracic cord injury of rodent, which was usually symmetrical [16,17]. This study, for the first time, evaluated and compared the alterations in the bone microstructures between ipsilateral and contralateral sides after unilateral cervical SCI in NHPs, the bone biomechanical properties muscle atrophy as well as the serological bone turnover markers were also analyzed.

The cervical SCI is common in clinic, while cntusion SCI model has been considered clinically relevant since contusion models appear to replicate the mechanism of the majority of human SCIs. Hemi-contusion SCI model reduces the mortality and complications of the experimental animals as the contralateral function is largely preserved and served as an internal control. On the other hand, Our understanding about pathology and therapeutic effects of SCI mostly came from rodents, which is limited

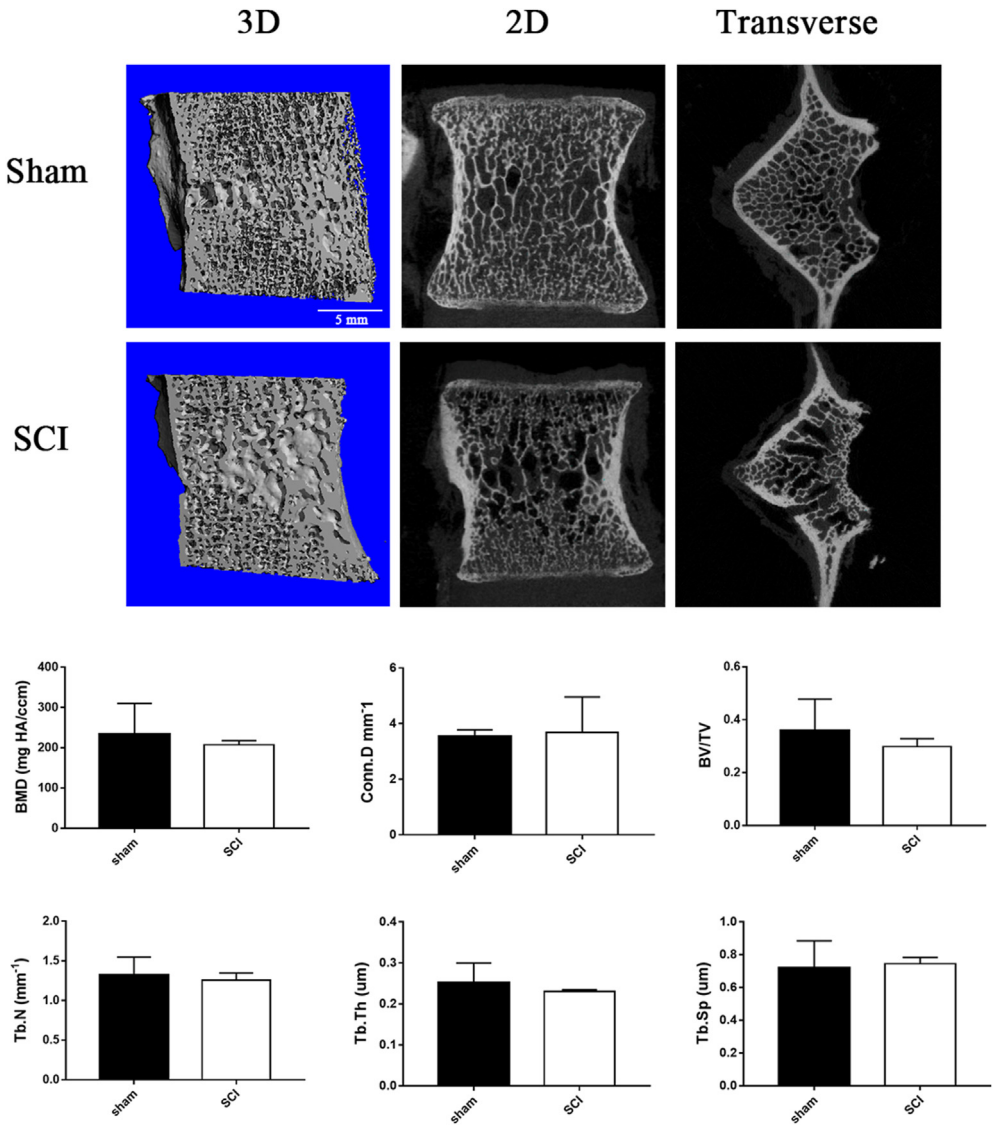

Fig. 5. The bone microstructure change of cancellous bone in L4.

when extrapolated to clinic, even to NHP. There are significant difference in specific motor tasks or anatomical and functional organization of the sensorimotor systems between rodents and primates . Therefore, it is worthy to verify the SCI pathology using NHP. A unilateral cervical spinal cord contusion injury model in NHPs (*Macaca mulatta*) has been established recently [11,13]. The spinal cord and central nervous system in NHP closely resemble humans, especially in consideration of the forelimb/hand function after cervical injuries [11]. Due to distinct differences between rodent and primate spinal cord systems in size, anatomy, inflammatory, previous studies identified the major differences between rodents and NHP with respect to corticospinal tract function and plasticity after injury using an NHP cervical spinal cord hemi-section model [18]. *Salegio* et al. successfully established a unilateral cervical spinal cord contusion injury model in NHPs, a large lesion in the ipsilateral spinal cord that affected both white matter and gray matter areas were found during the research [11]. Meanwhile, electrophysiological nerve evaluations, including MEPs and SEPs, have been widely used to assess the neurological function in SCI models [19,20]. Our previous study also monitored longitudinal electrophysiological changes after hemi-contusion cervical SCI in rats and found latency prolongation and amplitude reduction in the MEPs and SEPs of ipsilateral forelimbs after injury [21]. The present study is based on the previous research [13], the spinal cord lesions were observed in the ipsilateral epicenter after operation, latency prolongation and amplitude reduction of MEPs and SEPs were also in concordance with our previous research, and the results of the behavioral scoring, MRI, hematoxylin and eosin (H&E) staining, thus the successful establishment of the hemi-contusion cervical SCI model was confirmed.

According to previous research, SCI is usually associated with sublesional muscle atrophy [22] as well as transformation in the type of muscle fibers [23] in addition to electrophysiological changes. In a rodent spinal cord transection model, a 20–40% decrease was observed in the extensor muscles of the hind-limb, which also demonstrated a tendency to return to the control level after 30–60 days [24]. While another research revealed that spinal cord contusion in rats may result in a maximal 25% decrease in muscle weight after 1 week, which could not normalize even after 10 weeks [25]. Interestingly, after SCI, humans also exhibited significant muscle atrophy similar to animals. *Shah* et al. [26] demonstrated that individuals with incomplete SCI (5–37 months after injury) undergo marked atrophy of all the affected lower extremity muscles with 24% (tibialis anterior) to 31% (quadriceps femoris) decrease in cross-sectional area (CSA) of affected muscles. While *Gorgey AS* [22] reported that following 6 weeks of incomplete SCI, thigh CSA was observed to be 33% smaller compared to healthy controls. In the

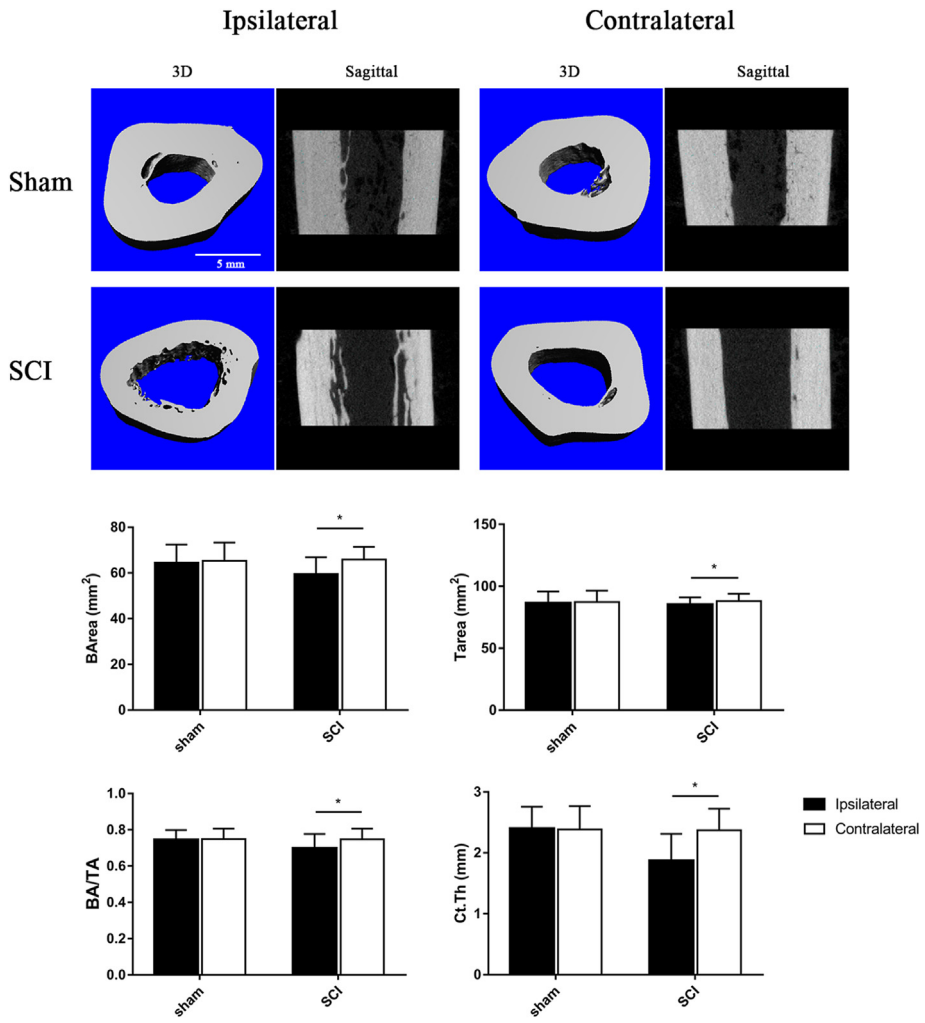

Fig. 6. The bone microstructure change of cortical bone in the mid-shaft humerus. **A** The 3D images of transverse section and the 2D images of sagittal section. B The parameters of cortical bone. *P < 0.05 between the ipsilateral side and contralateral side (control, n = 4; SCI, n = 8)

present study, after hemi-contusion cervical SCI in the NHPs, we found that all the affected forelimb muscles, including the MPL, FCR, PT, and BR on the contusion side were decreased by 36.8%, 39.8%, 52.3%, and 32.4% respectively as compared to the contralateral side. Our results were similar to but inconsistent with previous studies. We found that the weight of the forelimb muscles on the uninjured side in the SCI group was similar to that of the Sham group, indicating unilateral SCI may only result in unilateral muscle atrophy, which has been scarcely reported in previous researches.

An altered musculoskeletal system can be correlated directly to motor dysfunctions after SCI. *Lin* et al. [27] found that the average CSA of myofiber in the hindlimbs was associated with the level of locomotor activity. In motor complete SCI, the long bones of the lower extremities adapt to minimal mechanical strain via atrophy, osteoporosis is thus an inevitable complication, occurring predominantly in the pelvis and the lower extremities [28]. The pathogenesis of osteoporosis after SCI is generally considered to be disuse and immobilization [29], which may lead to muscle atrophy together with long-term denervation [30]. The decline in bone mineral density and bone mineral content have been documented in both acute and chronic SCI patients [31,32]. It may occur rapidly in the acute phase after injury and continue to decline until 2–3 years post-injury [33]. More importantly, in addition to sympathetic neural fibers [22], functional noradrenaline and various neuropeptide receptors have also been identified in bone cells [34,35], thus previous studies suggested that bone remodeling could also be regulated by nerve-derived signals, indicating sympathetic innervation might play a major role in bone function [36,37]. In our research, after hemi-contusion SCI, the muscles of forelimb exhibited marked atrophy, the bone mass of the humerus and radius decreased by 40.8% and 33.3% in the ipsilateral side compared to the contralateral side in the SCI group. Though without significance, the L4 vertebra also decreased by 16.9%. These results were consistent with the previous study that the bone mass of the sublesional extremities was reduced by 19–65% after thoracic spinal cord injury [17]. Clinically, in paralytic patients after SCI, fractures mainly occur in the lower extremities but not the spine, patients with incomplete lesions usually have the same bone mineral density (BMD) as uninjured persons in vertebrae [32], which may help explain the unchanged vertebra in our study.

Factors that contribute to SCI-induced bone loss may also include metabolic changes in addition to unloading and immobilization. During the early stage of SCI, skeletal changes result from a marked enhancement of bone resorption coupled with a lack of bone anabolic activity, as was evident by altered circulating markers of bone metabolism [28,37]. N-terminal propeptide of type I procollagen (PINP) and C-telopeptide of type I collagen (CTX) are typical markers of bone formation and resorption [38]. The largest bone turnover marker study showed a correlation between the serum levels of PINP and histomorphometric estimation of the bone formation and between CTX-I and bone resorption [39]. In the present study, the serological β-CTX level increased by 12.5% while the t-P1NP decreased by 48.6% after SCI, which proved that spinal

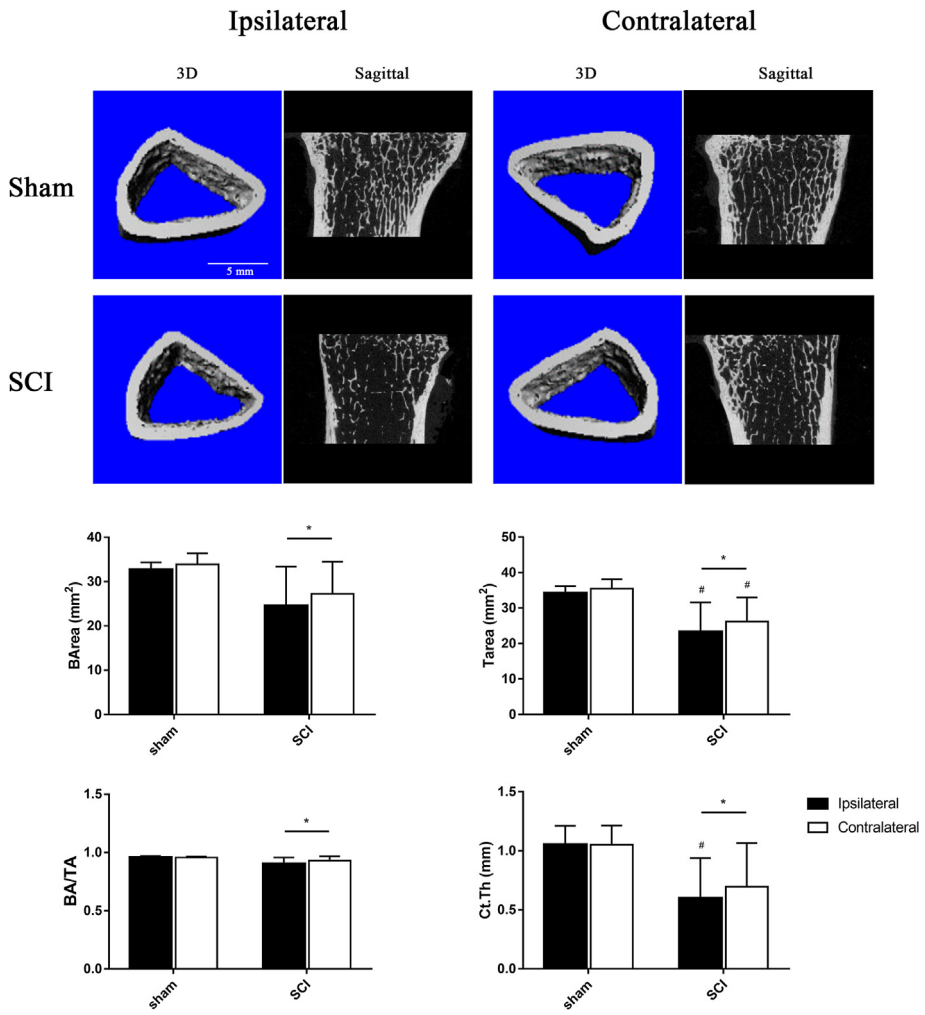

Fig. 7. The bone microstructure change of cortical bone in the distal radius.

Table 2
The biomechanical properties of humerus, radius and vertebrae measured by micro-FE.

		Stiffness ($\times 10^3$ N/mm)		Failure load ($\times 10^2$ N)	
		Sham	SCI	Sham	SCI
Humerus	Ipsilateral	210.6 ± 45.8	134.3 ± 26.9*#	34.5 ± 5.9	24.0 ± 4.1*#
	contralateral	214.3 ± 43.2	188.5 ± 20.4	35.4 ± 5.7	31.7 ± 3.0
Radius	Ipsilateral	116.8 ± 21.9	86.9 ± 32.4*	19.6 ± 3.5	10.1 ± 3.5*#
	contralateral	126.6 ± 26.2	133.0 ± 30.4	21.3 ± 4.2	16.7 ± 3.8
Vertebrae		41.2 ± 9.2	32.7 ± 1.5	2.2 ± 0.7	2.0 ± 0.2

Note: Data are expressed as means ± SD. *P < 0.05 between ipsilateral and contralateral sides in the SCI group; #P < 0.05 between the sham and SCI groups in the ipsilateral side (n = 4 and n = 8 in the humerus and radius in the sham and SCI groups; n = 4 in the vertebrae in the sham and SCI groups)

contusion probably switched bone metabolism from osteogenesis to osteoclasia. Moreover, osteoblasts express the maximal concentration of collagen during the proliferative phase: bone alkaline phosphatase (BALP) during matrix maturation and osteocalcin (OCN) during mineralization [40]. The serological OCN in our study reduced by 34.1% after SCI, which was consistent with the research by *Lin* et al. [17] that the serum concentration of OCN decreased dramatically after SCI in rats. However, *Sabour* et al. [41] found that there is no significant correlation between BALP and BMD at the chronic stage of SCI, which might be attributed to the plateau stage achieved in the bone formation process. Furthermore, the concentration of BALP in this study increased slightly after SCI. Researchers believed that imbalance between bone resorption and repair below the lesion might be due to low blood perfusion, venous stasis, and tissue acidosis [42], whose underlying mechanism needs further investigation. While in our study, although the bone turnover markers exhibited bone metabolic change from anabolism to catabolism, no significant difference was found between the sham and SCI groups, which may result from the increased false-negative rates owing to the limited number of *M. fascicularis*.

Table 3
The Calcium, Phosphorus and Vitamin D, and the biomarkers of bone metabolic in serum between sham and SCI groups.

	Calcium (mmol/L)	Phosphorus (mmol/L)	Vitamin D (ng/ml)	ALP (mmol/L)	OCN (U/L)	t-P1NP (U/L)	β-CTX (U/L)
Sham	2.2 ± 0.1	1.0 ± 0.1	122.3 ± 16.1	140.7 ± 40.3	11.5 ± 0.7	821.7 ± 380.6	1.0 ± 0.3
SCI	2.3 ± 0.1	1.7 ± 0.2	118.0 ± 18.5	163.0 ± 56.7	7.6 ± 2.0	422.1 ± 151.1	1.3 ± 0.2

Note: Data are expressed as means ± SD (n = 4 in the sham and SCI groups)

Another factor that induced bone loss after SCI could be sensory denervation. Chen et al. [43] demonstrated that knockout of the EP4 gene in the sensory nerves significantly reduces the number of osteocalcin positive osteoblasts as well as serum level of osteocalcin, whereas the number of tartaric acidic phosphatase (TRAP) positive osteoclasts and the level of osteoclast bone resorption marker carboxy-terminal collagen crosslinks did not change significantly. They also found that bone loss was more severe in 12-week-old TrkAAvil−/− mice than that in the wildtype littermates through μCT analysis. Furthermore, in our previous study [13], we found that there was no ipsi-contra difference in size frequency distributions of neurons from 48 wpi monkeys, but a clear rightward shift in injured monkeys compared with uninjured controls neuronal vacuolation, and neuronophagy were goning after hemi-contusion. In the present study, we also found that loss of bone mass on the ipsilateral side could be induced by hemi-SCI. Therefore, the results suggested that sensory denervation reduces osteoblastic bone formation may also play a role in SCI-induced bone loss.

Although whether the bone mass predicts bone strength is yet controversial, the results of both the actual biomechanical tests and the micro-FE analysis revealed a similar biochemical quality of the bone [44]. Our study carried out a simulated compressive test using micro-FE to evaluate the biomechanical properties of the bone, in which we found the loss of trabecular bone and deterioration of bone structure led to diminished stiffness (28.9% and 36.6%) and failure load (27.2% and 40.2%) in the humerus and radius on the ipsilateral side compared to the contralateral side after SCI, indicating a potentially higher rate of fractures on the upper extremities of injured side after hemi-cervical cord injury.

Several limitations of the study should also be mentioned. First, only 12 *M. fascicularis* were available in this study, the limited number of samples would cause a bias. Second, the present study only assessed the changes of bone mass in the forelimbs and vertebrae, the lower extremities should also be included to identify the effects of SCI on the entire skeleton. Moreover, histological staining of bone metabolism was not tested as specific monkey-related reagents was not available to us.

In conclusion, this comprehensive study demonstrated that hemi-cervical cord injury had deleterious effects on the ipsilateral of forelimbs, it may lead to deterioration of bone microstructure, reduction of bone mineral density, and weakness of bone mechanical properties. These changes were accompanied by muscle atrophy, sensory denervation and possibility of bone metabolism change from osteogenesis to bone resorption, but the mechanism is still unclear. Subsequent research should further extend, in particular, the relationship between nerves and osteoporosis.

Compliance with ethical standards

The protocol of the study was approved by the Ethics Committee of Southern Medical University.

Author disclosure statement

Xiuhua Wu, Xiaolin Xu, Qi Liu, Jianyang Ding, Junhao Liu, Zhiping Huang, Zucheng Huang, Xiaoliang Wu, Rong Li, Zhou Yang, Hui Jiang, Jie Liu and Qingan Zhu declare no competing financial interests.

Declaration of competing interest

A conflict of interest occurs when an individual's objectivity is potentially compromised by a desire for financial gain, prominence, professional advancement or a successful outcome. The Editors of the *Journal of Orthopaedic Translation* strive to ensure that what is published in the Journal is as balanced, objective and evidence-based as possible. Since it can be difficult to distinguish between an actual conflict of interest and a perceived conflict of interest, the Journal requires authors to disclose all and any potential conflicts of interest.

A The 3D images of transverse section and the 2D images of transverse and sagittal sections. B The trabecula parameters of cancellous bone (control, n = 4; SCI, n = 4).

A The 3D images of transverse section and the 2D images of sagittal section. B The parameters of cortical bone. *P < 0.05 between the ipsilateral side and contralateral side (control, n = 4; SCI, n = 8).

Acknowledgments

This study was supported by grants from the Provincial Science and Technology Plan Project of Guangdong Province (2017B090901051), the Rick Hansen Institute of Canada (PSRTC-2014-08) the National Natural Science Foundation of China (81972064), President Foundation of Nanfang Hospital, Southern Medical University (No.2017C041)and (No.2017H009).

References

[1] Bauman WA, Cardozo CP. Osteoporosis in individuals with spinal cord injury. Pharm Manag PM R 2015;7(2):188–201. quiz 01.
[2] Lacombe J, Cairns BJ, Green J, Reeves GK, Beral V, Armstrong MEG, et al. The effects of age, adiposity, and physical activity on the risk of seven site-specific fractures in postmenopausal women. J Bone Miner Res 2016;31(8):1559–68.
[3] Edwards WB, Schnitzer TJ, Troy KL. Bone mineral and stiffness loss at the distal femur and proximal tibia in acute spinal cord injury. Osteoporos Int 2014;25(3):1005–15.
[4] Gifre L, Vidal J, Carrasco J, Portell E, Puig J, Monegal A, et al. Incidence of skeletal fractures after traumatic spinal cord injury: a 10-year follow-up study. Clin Rehabil 2014;28(4):361–9.
[5] Jiang SD, Jiang LS, Dai LY. Mechanisms of osteoporosis in spinal cord injury. Clin Endocrinol 2006;65(5):555–65.
[6] Giangregorio L, McCartney N. Bone loss and muscle atrophy in spinal cord injury: epidemiology, fracture prediction, and rehabilitation strategies. J Spinal Cord Med 2006;29(5):489–500.
[7] Singh A, Tetreault L, Kalsi-Ryan S, Nouri A, Fehlings MG. Global prevalence and incidence of traumatic spinal cord injury. Clin Epidemiol 2014;6:309–31.
[8] Zhang N, Fang M, Chen H, Gou F, Ding M. Evaluation of spinal cord injury animal models. Neural Regen Res 2014;9(22):2008–12.
[9] Otzel DM, Conover CF, Ye F, Phillips EG, Bassett T, Wnek RD, et al. Longitudinal examination of bone loss in male rats after moderate-severe contusion spinal cord injury. Calcif Tissue Int 2019;104(1):79–91.
[10] Sparrey CJ, Salegio EA, Camisa W, Tam H, Beattie MS, Bresnahan JC. Mechanical design and analysis of a unilateral cervical spinal cord contusion injury model in non-human primates. J Neurotrauma 2016;33(12):1136–49.
[11] Salegio EA, Bresnahan JC, Sparrey CJ, Camisa W, Fischer J, Leasure J, et al. A unilateral cervical spinal cord contusion injury model in non-human primates (Macaca mulatta). J Neurotrauma 2016;33(5):439–59.
[12] Lee JH, Streijger F, Tigchelaar S, Maloon M, Liu J, Tetzlaff W, et al. A contusive model of unilateral cervical spinal cord injury using the infinite horizon impactor. JoVE 2012;65.
[13] Liu J, Li R, Huang Z, Huang Z, Li Y, Wu X, et al. A cervical spinal cord hemi-contusion injury model based on displacement control in non-human primates (Macaca fascicularis). J Neurotrauma 2020;37:1669–86. https://doi.org/10.1089/neu.2019.6822.
[14] Liu Q, Xu X, Yang Z, Liu Y, Wu X, Huang Z, et al. Metformin alleviates the bone loss induced by ketogenic diet: an in vivo study in mice. Calcif Tissue Int 2019;104(1):59–69.
[15] Lazo MG, Shirazi P, Sam M, Giobbie-Hurder A, Blacconiere MJ, Muppidi M. Osteoporosis and risk of fracture in men with spinal cord injury. Spinal Cord 2001;39(4):208–14.
[16] Lin CY, Androjna C, Rozic R, Nguyen B, Parsons B, Midura RJ, et al. Differential adaptations of the musculoskeletal system after spinal cord contusion and transection in rats. J Neurotrauma 2018;35(15):1737–44.
[17] Lin T, Tong W, Chandra A, Hsu SY, Jia H, Zhu J, et al. A comprehensive study of long-term skeletal changes after spinal cord injury in adult rats. Bone Res 2015;3:15028.
[18] Nout YS, Rosenzweig ES, Brock JH, Strand SC, Moseanko R, Hawbecker S, et al. Animal models of neurologic disorders: a nonhuman primate model of spinal cord injury. Neurotherapeutics 2012;9(2):380–92.
[19] Nicaise C, Frank DM, Hala TJ, Authelet M, Pochet R, Adriaens D, et al. Early phrenic motor neuron loss and transient respiratory abnormalities after unilateral cervical spinal cord contusion. J Neurotrauma 2013;30(12):1092–9.
[20] Hu Y, Wen CY, Li TH, Cheung MM, Wu EX, Luk KD. Somatosensory-evoked potentials as an indicator for the extent of ultrastructural damage of the spinal cord after chronic compressive injuries in a rat model. Clin Neurophysiol 2011;122(7):1440–7.
[21] Huang Z, Li R, Liu J, Huang Z, Hu Y, Wu X, et al. Longitudinal electrophysiological changes after cervical hemi-contusion spinal cord injury in rats. Neurosci Lett 2018;664:116–22.
[22] Gorgey AS, Dudley GA. Skeletal muscle atrophy and increased intramuscular fat after incomplete spinal cord injury. Spinal Cord 2007;45(4):304–9.

[23] Castro MJ, Apple Jr DF, Hillegass EA, Dudley GA. Influence of complete spinal cord injury on skeletal muscle cross-sectional area within the first 6 months of injury. Eur J Appl Physiol Occup Physiol 1999;80(4):373–8.
[24] Durozard D, Gabrielle C, Baverel G. Metabolism of rat skeletal muscle after spinal cord transection. Muscle Nerve 2000;23(10):1561–8.
[25] Hutchinson KJ, Linderman JK, Basso DM. Skeletal muscle adaptations following spinal cord contusion injury in rat and the relationship to locomotor function: a time course study. J Neurotrauma 2001;18(10):1075–89.
[26] Shah PK, Stevens JE, Gregory CM, Pathare NC, Jayaraman A, Bickel SC, et al. Lower-extremity muscle cross-sectional area after incomplete spinal cord injury. Arch Phys Med Rehabil 2006;87(6):772–8.
[27] Zehnder Y, Luthi M, Michel D, Knecht H, Perrelet R, Neto I, et al. Long-term changes in bone metabolism, bone mineral density, quantitative ultrasound parameters, and fracture incidence after spinal cord injury: a cross-sectional observational study in 100 paraplegic men. Osteoporos Int 2004;15(3):180–9.
[28] Kiratli BJ, Smith AE, Nauenberg T, Kallfelz CF, Perkash I. Bone mineral and geometric changes through the femur with immobilization due to spinal cord injury. J Rehabil Res Dev 2000;37(2):225–33.
[29] Cisterna BA, Cardozo C, Saez JC. Neuronal involvement in muscular atrophy. Front Cell Neurosci 2014;8:405.
[30] Warden SJ, Bennell KL, Matthews B, Brown DJ, McMeeken JM, Wark JD. Quantitative ultrasound assessment of acute bone loss following spinal cord injury: a longitudinal pilot study. Osteoporos Int 2002;13(7):586–92.
[31] Sabo D, Blaich S, Wenz W, Hohmann M, Loew M, Gerner HJ. Osteoporosis in patients with paralysis after spinal cord injury. A cross sectional study in 46 male patients with dual-energy X-ray absorptiometry. Arch Orthop Trauma Surg 2001; 121(1–2):75–8.
[32] Garland DE, Stewart CA, Adkins RH, Hu SS, Rosen C, Liotta FJ, et al. Osteoporosis after spinal cord injury. J Orthop Res 1992;10(3):371–8.
[33] Lundberg P, Lie A, Bjurholm A, Lehenkari PP, Horton MA, Lerner UH, et al. Vasoactive intestinal peptide regulates osteoclast activity via specific binding sites on both osteoclasts and osteoblasts. Bone 2000;27(6):803–10.
[34] Bliziotes MM, Eshleman AJ, Zhang XW, Wiren KM. Neurotransmitter action in osteoblasts: expression of a functional system for serotonin receptor activation and reuptake. Bone 2001;29(5):477–86.
[35] Sandhu HS, Herskovits MS, Singh IJ. Effect of surgical sympathectomy on bone remodeling at rat incisor and molar root sockets. Anat Rec 1987;219(1):32–8.
[36] Hill EL, Turner R, Elde R. Effects of neonatal sympathectomy and capsaicin treatment on bone remodeling in rats. Neuroscience 1991;44(3):747–55.
[37] Reiter AL, Volk A, Vollmar J, Fromm B, Gerner HJ. Changes of basic bone turnover parameters in short-term and long-term patients with spinal cord injury. Eur Spine J 2007;16(6):771–6.
[38] Eastell R, Szulc P. Use of bone turnover markers in postmenopausal osteoporosis. Lancet Diabetes Endocrinol 2017;5(11):908–23.
[39] Chavassieux P, Portero-Muzy N, Roux JP, Garnero P, Chapurlat R. Response to the letter: are biochemical markers of bone turnover representative of bone histomorphometry in 370 postmenopausal women? J Clin Endocrinol Metab 2016; 101(2):L26.
[40] Stein GS, Lian JB. Molecular mechanisms mediating proliferation/differentiation interrelationships during progressive development of the osteoblast phenotype. Endocr Rev 1993;14(4):424–42.
[41] Sabour H, Norouzi Javidan A, Latifi S, Larijani B, Shidfar F, Vafa MR, et al. Bone biomarkers in patients with chronic traumatic spinal cord injury. Spine J 2014; 14(7):1132–8.
[42] Chantraine A. Actual concept of osteoporosis in paraplegia. Paraplegia 1978;16(1): 51–8.
[43] Chen H, Hu B, Lv X, Zhu S, Zhen G, Wan M, et al. Prostaglandin E2 mediates sensory nerve regulation of bone homeostasis. Nat Commun 2019;10(1):181.
[44] Comelekoglu U, Mutlu H, Yalin S, Bagis S, Yildiz A, Ogenler O. [Determining the biomechanical quality of normal and osteoporotic bones in rat femora through biomechanical test and finite element analysis]. Acta Orthop Traumatol Turcica 2007;41(1):53–7.